Proc. Natl. Acad. Sci. USA
Vol. 87, pp. 7410–7413, October 1990
Biophysics

Electron transfer to the binuclear center in cytochrome oxidase: Catalytic significance and evidence for an additional intermediate

(metalloproteins/kinetics/redox interactions/catalysis)

FRANCESCO MALATESTA*, PAOLO SARTI†, GIOVANNI ANTONINI*, BEATRICE VALLONE‡, AND MAURIZIO BRUNORI‡

*Department of Experimental Medicine and Biochemical Sciences, University of Rome "Tor Vergata," 00173 Rome, Italy; †Department of Biomedical Sciences, Technology and Biometry, University of L'Aquila, 67100 L'Aquila, Italy; and ‡Department of Biochemical Sciences and Center of Molecular Biology of the Consiglio Nazionale delle Ricerche, University of Rome "La Sapienza," 00185 Rome, Italy

Communicated by Harry B. Gray, June 25, 1990

ABSTRACT **We have followed, by transient kinetics, the reduction of cytochrome a_3 in the presence of carbon monoxide under different experimental conditions. We have observed that the internal electron transfer rate accounts for the turnover number, and both display the same pH and temperature dependence [$pK_a = 7.4$ and activation energy (E_a) = 14.7 ± 0.1 kcal/mol]. Moreover, comparison of the time course of cytochrome *c* oxidation and cytochrome a_3 reduction indicates that two electrons are transferred internally and with different rates to the oxygen-binding site. A kinetic model based on sequential internal electron transfer pathways, describing quantitatively the experimental data, is presented and discussed.**

Cytochrome *c* oxidase (EC 1.9.3.1) is a mitochondrial redox-linked proton pump, containing redox active metal centers involved in catalyzing electron transfer from cytochrome *c* to molecular oxygen (1–3). The electron transfer pathway(s) in between the various metals, though thoroughly studied, is only partially understood. A sequential mechanism, previously described (4), assumes that electron transfer from reduced cytochrome *c* to the enzyme proceeds via cytochrome *a*–Cu_A (the electron accepting pole) and that cytochrome a_3–Cu_B (the binuclear center, where reduction of O_2 to water takes place) is reduced intramolecularly. Transient kinetic data have indicated that the internal electron transfer to the binuclear center is the rate-limiting step during turnover (5); on the other hand, steady-state kinetic data have indicated that the rate of cytochrome c^{3+} dissociation from specific binding site(s) on the enzyme is rate-determining (6), although this interpretation has been challenged (ref. 7 and references therein).

In a classical paper, Gibson *et al.* (8) reported the first unequivocal determination of the internal electron transfer to the binuclear center by monitoring the rate of formation of cytochrome a_3^{2+}–CO using a flow-flash technique. A conceptually similar experimental design has been extensively used in the present paper, in order to correlate the turnover number and the internal electron transfer process over a wide range of experimental conditions (including pH, temperature, and detergent). We conclude that indeed an internal kinetic step leading to reduction of cytochrome a_3 correlates extremely well with the initial rate of cytochrome c^{2+} oxidation in air. Moreover, comparison of the time course of cytochrome c^{2+} oxidation with that of cytochrome a_3 reduction reveals an unexpected feature, relevant to the pathway of reduction of the two metal centers in the binuclear cluster. A scheme describing quantitatively the internal electron transfer to the binuclear center is presented.

The publication costs of this article were defrayed in part by page charge payment. This article must therefore be hereby marked "*advertisement*" in accordance with 18 U.S.C. §1734 solely to indicate this fact.

MATERIAL AND METHODS

Cytochrome *c* oxidase was purified from ox heart according to Yonetani (9), with minor modifications. The concentration of the enzyme is expressed in functional (monomeric) units and was determined spectroscopically by using $\Delta\varepsilon$ = 22 $mM^{-1}\cdot cm^{-1}$ (reduced − oxidized) at 605 nm (9). Type VI cytochrome *c* was from Sigma. All reagents were of analytical grade. Static spectra were collected with a Cary 219 or an Olis-converted Cary 14 spectrophotometer (On Line Instrument Systems, Jefferson, GA). Stopped-flow experiments were carried out by using a thermostatted Durrum-Gibson stopped-flow apparatus (dead time = 4 ms) equipped with a 2-cm pathlength observation chamber and interfaced to a Compaq 286 computer for data collection (1000 data points per record) and analysis. Unless otherwise stated, all concentrations are expressed after mixing. A typical experiment was carried out as follows: 20 μM cytochrome oxidase, and 100 μM cytochrome *c* solubilized either in Hepes buffer (1–5 mM) or in higher ionic strength buffers (see below), all containing 0.5% Tween 80, were carefully degassed, equilibrated with nitrogen, and fully reduced with 1 mM sodium ascorbate directly in the driving syringe of the stopped-flow apparatus. The fully reduced enzyme was mixed with buffer containing 1 mM CO and oxygen stoichiometric or substoichiometric with the functional unit of cytochrome oxidase (four electron equivalents). CO binding to the fully reduced enzyme was determined independently for each experiment. In agreement with previous data (10), at any given CO concentration, the pseudo-first-order rate constants varied only with temperature.

The formation of the CO complex was followed in the spectral region of 570–610 nm; the best wavelength was found to be 585 nm. At this wavelength, the contribution of cytochrome *c* oxidation is about 30% of the total absorbance change. Relative contributions of the chromophores were determined independently under otherwise identical conditions. Corrections were carried out for data analysis. The oxidation of cytochrome *c* was followed at 563 nm [$\Delta\varepsilon$ (reduced − oxidized) = 3.5 $mM^{-1}\cdot cm^{-1}$], where the contribution of the spectral changes of cytochrome oxidase is ≈5%. The pH dependence of the reactions was determined with the following buffers: 0.1 M phosphate at pH 6.0–7.0, 0.1 M Hepes at pH 7.0–8.0, and 0.1 M Tris at pH values >8.0. Different pH values were obtained by mixing the 1 mM buffered protein with the above buffers, and the reported pH values were controlled on the outflow. The turnover number was calculated from the initial rate of cytochrome *c* oxidation in air, at 550 or 563 nm. The rate of oxygen consumption was determined by using a Clark type oxygen electrode (Ysi 3000, Yellow Springs Instruments).

Numerical solutions to the differential equations describing the kinetic mechanism (see below) were obtained with a

Compaq 286 computer (equipped with a mathematical coprocessor), using a program written in TURBO PASCAL (Borland, version 5.0). All numerical computations were carried out by using an integration step of 1 μs, and in any case the integration step was always at least 50 times smaller than the half-time of the fastest reaction step. In the present experiments, the bimolecular reaction for binding and oxidation of cytochrome *c* is $k_{on} = 10^8\ M^{-1}\cdot s^{-1}$; at 100 μM cytochrome *c* this yields a pseudo-first-order rate constant of $\approx 10^4\ s^{-1}$ and a half-time of about 70 μs.

RESULTS AND DISCUSSION

On mixing ascorbate-reduced cytochrome *c* and reduced cytochrome oxidase with stoichiometric oxygen containing 1 mM CO, a transient is clearly resolved in the visible spectral range; the same transient is not seen in the absence of CO. Fig. 1 shows the experimental time course at 563 and 585 nm, the wavelengths characteristic of, respectively, the oxidation of cytochrome *c* and the formation of the CO complex of ferrocytochrome a_3. The transient at 585 nm has been assigned to the reaction: cytochrome $a_3^{3+} \rightarrow$ cytochrome a_3^{2+}–CO, because the time course is independent of cytochrome c^{2+} concentration (from 25 to 100 μM) and CO concentration (from 0.1 to 0.5 mM), all after mixing. It should be noted (see also Fig. 5) that the experimental design is such that reduction of cytochrome a_3 is limiting the binding of CO. Experiments at 605 nm (not shown) yield a relatively small spectral change consistent with the contribution of the CO complex formation at this wavelength. This demonstrates that, when the observation starts, the reduction of cytochrome *a* (which makes the largest contribution at 605 nm, see ref. 1) is complete. This is expected because, given the concentrations of the reactants, reduced cytochrome oxidase should be fully oxidized by oxygen and half rereduced by the large excess of cytochrome c^{2+} within the dead time of the stopped-flow apparatus. It may be seen from Fig. 1 that the signal at 585 nm follows an exponential time course and the absorbance recovery is consistent with the expected formation of the CO complex. On the other hand, the oxidation of cytochrome *c* (at 563 nm) is biphasic, and the initial rate is approximately twice as fast as the formation of the cytochrome a_3^{2+}–CO complex; this feature will be discussed below. First-order kinetic analysis of the time course at 563 nm (see Fig. 1 *Inset*) shows that the initial phase accounts for the oxidation of $\approx$1 equivalent of cytochrome c^{2+} per oxidase

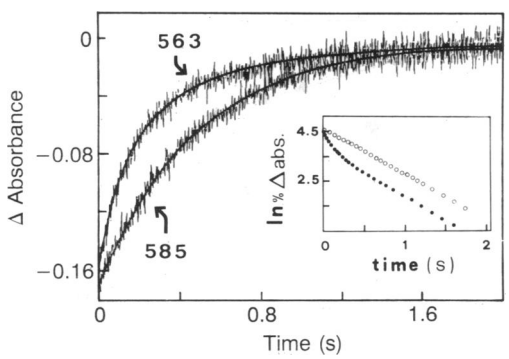

FIG. 1. Time course of oxidation of cytochrome *c* (563 nm) and formation of the CO complex of cytochrome oxidase (585 nm). Concentrations after mixing: cytochrome oxidase = 10 μM, cytochrome *c* = 50 μM, sodium ascorbate = 0.4 mM, oxygen $\approx$10 μM, CO = 0.5 mM. The buffer was 0.05 M sodium/potassium phosphate (pH 6.2) containing 0.5% Tween 80 at *t* = 7.5°C. (*Inset*) Semilogarithmic analysis of the 585 nm signal (○) and the 563 nm signal (●). Solid lines were obtained by a nonlinear Levenberg–Marquardt fitting algorithm. The fitted rate constants are 4.0 and 1.8 s^{-1} for the fast and slow phases at 563 nm and 2.0 s^{-1} at 585 nm, respectively.

functional unit, while the following exponential phase accounts for somewhat less than one additional equivalent of cytochrome *c* oxidized and proceeds at a rate very close to that observed at 585 nm (see Fig. 1 *Inset*). At 563 and 585 nm, oxidation of cytochrome *c* and binding of CO to cytochrome oxidase both contribute to the increase in absorbance, although to a significantly different extent. At 563 nm, 95% of the absorbance change is contributed by the oxidation of cytochrome c^{2+}, whereas at 585 nm the formation of the complex of cytochrome oxidase with CO contributes $\approx$70% of the total signal. At the latter wavelength, correction for the contribution of cytochrome *c* oxidation often indicates the presence of a perceptible lag phase followed by an exponential process (see Fig. 2).

The correlation between the slowest electron transfer step (leading to reduction of cytochrome a_3 and thus CO binding) and the turnover rate has been extensively investigated. Kinetic parameters have been compared under a number of different experimental conditions, including pH (from 6.2 to 8.9), temperature (from 7.5 to 34.5°C), and type of detergent (Tween 80 or Triton X-100 each at 1%). To illustrate the results, Fig. 2 shows the time courses, expressed as the percent change in absorbance at 585 and 563 nm, under two extreme conditions (i.e., pH 6.2 at 34.5°C in one case and pH 7.2 at 20°C in the presence of 1% Triton X-100 in the other). The signals at 585 nm have been corrected for the contribution of cytochrome *c* oxidation at this wavelength (see above). The calculated first-order rate constant for the internal electron transfer process in the former case is 17 s^{-1}, a value $\approx$40 times higher than that observed in the latter case (0.4 s^{-1}). The turnover number measured independently on the same material was 60 and 2 s^{-1}, respectively. Clearly, enhancement of the internal electron transfer rate constant parallels the increase of the turnover rate.

The dependence on pH of the internal electron transfer is shown in Fig. 3, where data obtained in turnover experiments are also reported. All the data points can be fitted with a single ionization group with a $pK_a = 7.4$, in good agreement with other estimates based on the pH dependence of catalytic activity (11). The correlation between internal electron transfer and turnover number also supports the consideration that the use of CO as a trapping ligand is justified. Moreover, it should be noted that the absolute values of the internal rate constant and the turnover number coincide, when the former values are multiplied by a factor of 4 (see the two ordinates in Fig. 3) to account for the stoichiometry. The activation energy for the internal electron transfer process and the turnover number, calculated from experiments carried out from 7.5 to 34.5°C, is essentially the same [activation energy (E_a) = 14.7 ± 0.1 kcal/mol], as shown in Fig. 4. The same figure shows that CO binding to the fully reduced enzyme is characterized by a clearly different activation energy: E_a = 6.8 kcal/mol, in agreement with previous results (10).

As reported above, the time course at 563 nm (yielding approximately two cytochrome c^{2+} oxidized per cytochrome oxidase functional unit) is always described by two kinetic phases; the absorbance change at 585 nm lags behind. These observations imply that an electron is transferred to the binuclear site more rapidly than binding of CO to cytochrome a_3. Thus, after the first two electrons (rapidly transferred to the enzyme in the burst phase and lost in the dead time, see Fig. 5), more cytochrome c^{2+} is oxidized, and reduction of cytochrome a_3–Cu_B (which is a prerequisite for the binding of CO) follows.

This observation provides some insight into the mechanism of intramolecular electron transfer in cytochrome oxidase. Electron transfer to the oxygen-binding site is usually considered to be a (concerted) two-electron process (12), and its rate was proposed to depend (for example) on the reduction of cytochrome *a* and Cu_A, leading to a conformationally

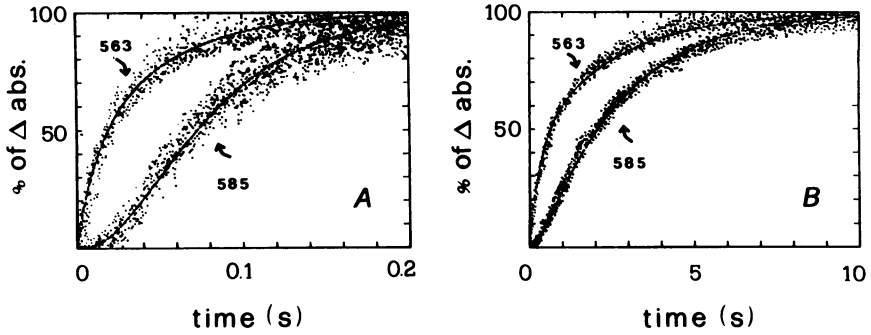

FIG. 2. Effect of solvent conditions and temperature on the electron transfer processes at 585 and 565 nm. (*A*) Experimental conditions were as in Fig. 1 except that t = 34.5°C. (*B*) Cytochrome oxidase (20 μM) was dissolved just before the experiment in 5 mM phosphate buffer (pH 7.0) containing 2% Triton X-100 and mixed with the same buffer without detergent. The cytochrome *c* concentration was 100 μM; other reactants were as in Fig. 1, t = 20°C. Correction for the contribution of cytochrome *c* oxidation (traces at 585 nm) was computed as outlined in *Materials and Methods*. The solid lines represent the simulations carried out with the model depicted in Fig. 5 and using the following set of parameters: cytochrome oxidase and cytochrome *c* concentrations, 10 and 100 μM, respectively; $k_0 = 10^8$ $M^{-1}\cdot s^{-1}$. (*A*) t = 34.5°C, $k_1 = 90$ s^{-1}, $k_2 = 20$ s^{-1}, $k_3 = 80{,}000$ $M^{-1}\cdot s^{-1}$. (*B*) t = 20°C, $k_1 = 3$ s^{-1}, $k_2 = 0.4$ s^{-1}, $k_3 = 70{,}000$ $M^{-1}\cdot s^{-1}$.

favorable partially reduced state (the so-called E2 or "open" conformation; refs. 13 and 14). There is, however, no direct evidence on the detailed mechanism for the internal two-electron transfer process. We will now present and discuss a kinetic model (shown in Fig. 5) that accounts for these experimental observations.

The top line in Fig. 5 shows the kinetic model and details the global (sum of their) oxidation states of the cytochrome *a*–Cu_A pair and the binuclear site, since each metal in a given pair, when reduced, rapidly exchanges the electron with its partner metal (11, 15–17). The second line in Fig. 5 shows in a schematic way the structure of each intermediate for rapid identification. The reaction is started by mixing the fully reduced enzyme (species A_0 in Fig. 5) with stoichiometric O_2, yielding the fully oxidized, pulsed oxidase. In view of the presence of excess cytochrome c^{2+} and favorable medium conditions, two electrons are very rapidly transferred to cytochrome *a* and Cu_A (step 0). Species A is therefore fully populated within the dead time of the stopped-flow apparatus, and experimental observation starts. In the simulations, A is the starting species for all numerical computations. The oxidation of cytochrome *c* (steps 2 and 4) is now rate-limited by the internal electron transfer from cytochrome *a*–Cu_A site(s) to the binuclear center (steps 1 and 3). The electrons in the present scheme are transferred sequentially to the binuclear site with different rates; the first internal electron transfer (step 1) negatively affects the rate of the second (step 3); therefore, k_1 is always greater than k_2. As known from binding data (10), once two electrons have been transferred to the cytochrome a_3–Cu_B site, the large excess of CO in the reaction medium ensures rapid trapping of the reduced enzyme and practically the irreversibility of step 5. The formal model implies that the electrons are transferred sequentially to the binuclear site taken as a unit. However, by reference to the structural features of the enzyme, the experimental time course may be equally well described by transfer of two electrons through parallel pathways, from Cu_A and cytochrome *a*, which are known to be in rapid redox equilibrium (15–17). The experimental traces obtained under the extreme conditions of Fig. 2 are compared with the simulations obtained by numerical integration of the differential equations that describe the kinetic mechanism (see Fig. 5). Simulations clearly indicate the presence of a lag phase at 585 nm, whose length may be sensitive to CO concentration since, at a given internal electron transfer rate, decreasing CO increases the length of this phase (results not shown). Nonetheless, it is clear that at the initial stages of the reaction, very little change is expected to occur at the wavelengths monitoring the CO binding to the binuclear site (species F). Indeed, in several experiments a lag phase was

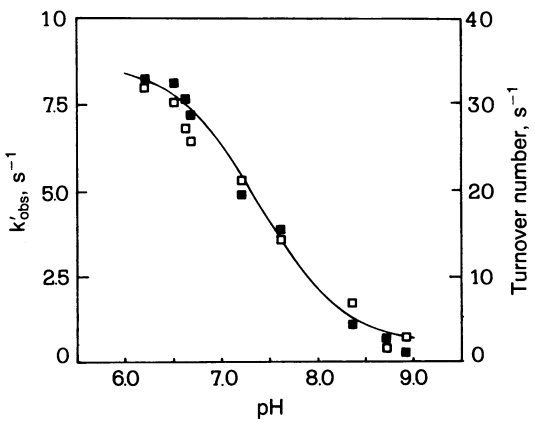

FIG. 3. pH dependence of the first-order rate constant for the formation of the CO complex (left ordinate) and of the turnover number (right ordinate). k_{obs} values were calculated from the semilogarithmic analysis of the time courses at 585 nm (■). Turnover numbers (□) were calculated from the initial slope of the time course of cytochrome *c* oxidation in air, after dilution of cytochrome oxidase to 2 μM. Other conditions were as in Fig. 1. t = 20°C.

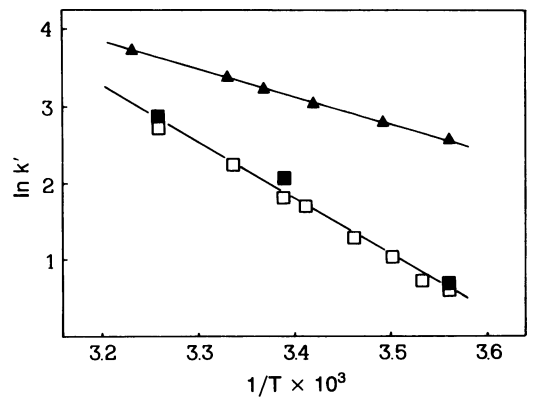

FIG. 4. Temperature dependence of the internal electron transfer (■), the turnover number (□), and binding of CO to fully reduced cytochrome oxidase (▲). Note that the first-order rate constant, k', for the internal electron transfer has been multiplied by 4, to account for one complete turnover (see text and ref. 5); other conditions were as in Fig. 1. Turnover numbers were calculated as in Fig. 3. The CO binding reaction was followed at 585 nm by mixing fully reduced cytochrome oxidase with 1 mM CO, in the absence of O_2.

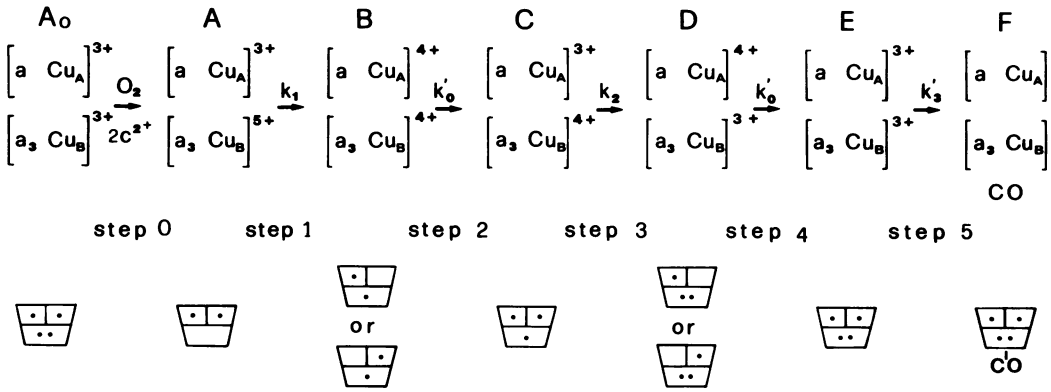

FIG. 5. Kinetic model for the internal electron transfer in cytochrome oxidase. The model used for the simulations is presented as a series of sequential irreversible steps from fully reduced to the fully reduced CO compound of cytochrome oxidase, because (under the experimental conditions used) the reaction is strongly driven to the right. Simulations carried out with a model where steps 1 and 3 were made reversible (with values of $k_{-1} = k_{-2}$ ranging from 0.1 to 500 s^{-1}) gave results identical to those shown in Fig. 2. The rate constant for binding and oxidation of cytochrome *c* is given as a pseudo-first-order rate constant $k_0' = k_0 \cdot [c^{2+}]$ where, at any time, $[c^{2+}]$ indicates the instantaneous ferrocytochrome *c* concentration. The corresponding pseudo-first-order rate constant for CO binding is $k_3' = k_3 \cdot [CO]$. The fully reduced CO complex of the enzyme (species F, 585-nm signal) and ferricytochrome *c* (563-nm signal) are the two species plotted in the simulations, compared in Fig. 2 with experimental data.

seen directly at 585 nm and more clearly so after correction for the contribution of cytochrome *c* (see Fig. 2). The length of this lag phase should partially overlap with the fast phase at 563 nm, and clearly indicates that more than one electron is required for CO binding. This feature is in agreement with redox titrations of the binuclear site in the presence of CO, which indicated a cooperative reduction process, with a value of $n = 2$ (18), consistently with the very close proximity of cytochrome a_3 and Cu_B. Thus, a one-electron reduced binuclear site will not bind CO (and possibly O_2) even if the electron were to reside on cytochrome a_3. A possible explanation of this phenomenon may lie in the reduced charge on the iron of cytochrome a_3 due to electron delocalization to the vicinal Cu_B; however, the reverse situation may be equally likely. A possible structure of the one-electron reduced binuclear site (species B and C in Fig. 5) may therefore be represented as in the following scheme:

$$[a_3^{2+} - Cu_B^{2+} \leftrightarrow a_3^{3+} - Cu_B^{+}],$$

and we believe it has been detected for the first time in the present experiments. Further work is needed to determine its spectroscopic and kinetic properties.

We thank Mr. Emilio D'Itri for skillful technical assistance. This work was partially supported by a grant from the Ministero dell'Universita' e della Ricerca Scientifica e Tecnologica of Italy and by the Consiglio Nazionale delle Ricerche (Progetto Finalizzato Biotecnologie e Biostrumentazioni).

1. Wikström, M., Krab, K. & Saraste, M. (1981) in *Cytochrome Oxidase: A Synthesis* (Academic, London).
2. Chan, S. I. & Li, P. M. (1990) *Biochemistry* **29**, 1–12.
3. Brunori, M., Antonini, G., Malatesta, F., Sarti, P. & Wilson, M. T. (1988) *Adv. Inorg. Biochem.* **7**, 93–153.
4. Wilson, M. T., Peterson, J., Antonini, E., Brunori, M., Colosimo, A. & Wyman, J. (1981) *Proc. Natl. Acad. Sci. USA* **78**, 7115–7122.
5. Sarti, P., Antonini, G., Malatesta, F., Vallone, B. & Brunori, M. (1988) *Ann. N.Y. Acad. Sci.* **550**, 161–166.
6. Ferguson-Miller, S., Brautigan, D. L. & Margoliash, E. (1976) *J. Biol. Chem.* **251**, 1104–1115.
7. Michel, B. & Bosshard, H. R. (1989) *Biochemistry* **28**, 244–252.
8. Gibson, Q. H., Greenwood, C., Wharton, D. H. & Palmer, G. (1965) *J. Biol. Chem.* **240**, 888–894.
9. Yonetani, T. (1961) *J. Biol. Chem.* **236**, 1680–1688.
10. Gibson, Q. & Greenwood, C. (1963) *Biochem. J.* **86**, 541–554.
11. Brzezinski, P. & Malmström, B. G. (1987) *Biochim. Biophys. Acta* **894**, 29–38.
12. Antonini, E., Brunori, M., Greenwood, C. & Malmström, B. G. (1970) *Nature (London)* **228**, 936–937.
13. Malmström, B. G. (1989) *FEBS Lett.* **250**, 9–21.
14. Gray, H. B. & Malmström, B. G. (1989) *Biochemistry* **28**, 7499–7505.
15. Greenwood, C., Brittain, T., Wilson, M. T. & Brunori, M. (1976) *Biochem. J.* **157**, 591–598.
16. Antalis, T. M. & Palmer, G. (1982) *J. Biol. Chem.* **257**, 6194–6206.
17. Kobayashi, K., Une, H. & Hayashi, K. (1989) *J. Biol. Chem.* **264**, 7976–7980.
18. Lindsay, J. G., Owen, C. S. & Wilson, D. F. (1975) *Arch. Biochem. Biophys.* **169**, 492–505.